A Fast and Accurate Chirp Rate Estimation Algorithm Based on the Fractional Fourier Transform

Ahmet Serbes
Department of Electronics and Communications Engineering
Davutpasa, Istanbul, 34220, Turkey
Email: aserbes@yildiz.edu.tr

Omair Aldimashki
Department of Electronics and Communications Engineering
Davutpasa, Istanbul, 34220, Turkey
Email: omair@dleaf.com

***Abstract*—In this work, a fast and accurate chirp-rate estimation algorithm is presented. The algorithm is based on the fractional Fourier transform. It is shown that utilization of the golden section search algorithm to find the maximum magnitude of the fractional Fourier transform domains not only accelerates the process, but also increases the accuracy in a noisy environment. Simulation results validate the proposed algorithm and show that the accuracy of parameter estimation nearly achieves the Cramer-Rao lower bound for SNR values as low as -7dB.**

***Index terms*—** Chirp signals, fractional Fourier transform, chirp rate, golden section search.

I. Introduction

Chirp signals are widely used in radar [1], sonar [2], aerospace [3], ultrasound [4], communication [5] and many other areas. A mono-component chirp signal can be described as a signal whose frequency may increase or decrease linearly over time. A chirp signal embedded in noise can be defined as

$$f(t) = A\exp\left[j\pi\left(mt^2 + 2f_0 t + \varphi_0\right)\right] + w(t), \qquad (1)$$

where A, m, f_0, and φ_0 represent amplitude, chirp rate, initial frequency, and initial phase, respectively. The additive white Gaussian noise (AWGN) with variance σ^2 is represented by $w(t)$. Many studies have been directed towards the development of techniques that would suffice to estimate the chirp parameters accurately in noisy environments. For many applications, only certain parameters are of interest. This paper is only interested in estimating the chirp rate. Earlier methods for estimating the chirp-rate depend on using a maximum likelihood estimator (MLE) [6]. Although it is very precise, the need for a multi-dimension search makes it computationally demanding. Due to the time varying characteristic of chirp signal, time-frequency-based methods are considered later, such as short-term Fourier transform (STFT) [7], [8], Wigner-Ville distribution (WVD) [9] and Radon-Wigner distribution (RWD) [10]. Even though the complexity of STFT computation is low, estimation performance is not satisfactory due to its poor time-frequency resolution. With its high immunity to noise and superior time-frequency localization, WVD-based methods have been also employed [11], [12]. However, they are not suitable for most practical applications, because of their high computational complexity.

The fractional Fourier transform (FrFT) has found many applications in various areas. Application of FrFT-based algorithms to the problem of estimating chirp parameters achieves good performance [13]. In the FrFT domains, there is an optimum transform angle associated with the chirp rate, which concentrates the energy and keeps the signal compact. At this angle, the signal is transformed to an impulse with a maximum magnitude [14], [15]. Therefore, searching for the maximum magnitude in the FrFT domains allows us to estimate the chirp rate. Zheng and Shi [16] use the idea of maximum magnitude of the FrFT domains for estimating a compact fractional Fourier domain. In order to reduce the computational complexity, they propose a coarse-to-fine grid-search strategy.

This paper proposes a fast and accurate method for estimating chirp rates in noisy environments based on the FrFT and the golden section search algorithm (GSS). Performance of the proposed algorithm has been evaluated using computer simulations. The results of the simulations show that the proposed method achieves higher performance in comparison with the method used by Zheng and Shi [16] while incurring reduced computational cost. The proposed method nearly achieves the Cramer-Rao lower bound (CRLB) at lower SNR values.

The rest of the paper is organized as follows. Section II introduces the FrFT briefly and then gives introductory information about the chirp-rate estimation problem in the FrFT domains. Section III introduces and discusses the proposed algorithm for estimating chirp rates in the FrFT domains in detail. The proposed algorithm is validated in Section IV, where simulation results are given. The paper is concluded in Section V.

II. Background

In this section the FrFT is briefly introduced. Then, a robust method employed in [13], [16] for estimating the chirp-rate by using the FrFT is reviewed.

ISBN 978-0-9928626-7-1

A. The Fractional Fourier Transform

The FrFT is a generalization of the ordinary Fourier transform (FT) [17], where the ordinary FT is a special case of the FrFT. It is natural that the generalized form will enlarge the circle of applications that can be utilized. Examples of these applications include time-variant filtering and multiplexing [18], solution of differential equations [19], applications of time-frequency distributions [20], pattern recognition [21], and many others.

In the time-frequency plane, the FrFT acts as a counterclockwise rotation of the axes around the origin of the coordinates. Therefore, the ordinary FT can be interpreted as a rotation from time to frequency axis, in which the rotation angle is $\frac{\pi}{2}$. As a generalization, the FrFT is considered as a rotation of the time-frequency axis by an angle of α. The FrFT of a signal $f(t)$ at the angle α is defined as

$$f_\alpha(u) = F^\alpha[f(t)] = \int_{-\infty}^{+\infty} f(t)\, K_\alpha(t,u)\, dt, \tag{2}$$

where α is the transform angle. $K_\alpha(t,u)$ is the kernel defined by

$$K_\alpha(t,u) = \begin{cases} A_\alpha e^{j\pi\left(t^2\cot\alpha + u^2\cot\alpha - tu\csc\alpha\right)}, & \alpha \neq n\pi \\ \delta(t-u), & \alpha = 2n\pi \\ \delta(t+u), & \alpha = (2n\pm 1)\pi \end{cases}. \tag{3}$$

Here, $A_\alpha = \sqrt{1 - j\cot\alpha}$ and n is any integer. Obviously, the FrFT transforms the signal to another domain, u domain, which is called the FrFT domain. The ordinary FT can be obtained by setting $\alpha = \frac{\pi}{2}$ and $\alpha = 0$ results in the signal itself. Consequently, time and frequency domains are simply special cases of the FrFT [22]. Assigning other values to α results in rotated time frequency representation of the signal. Therefore, the FrFT can be presumed to be an interpolation between the signal $f(t)$ and its FT.

B. Chirp Rate Estimation in the Fractional Fourier Domains

Time-frequency distribution of a chirp signal is a straight line making an angle associated with its chirp-rate in time-frequency domain as seen in Figure 1-a. The FrFT is an energy-preserving transform that can be applied to a signal with a continuous angle of rotation as shown in Figure 1-b. By applying a variable rotation angle, there are some angles in which the signal gets more compact in the transform domain. As the signal gets compact, the magnitude increases for some values of u as a result of preservation of the energy through the transformation. Therefore, any chirp signal can be transformed into a impulse, where the signal's energy is concentrated to the smallest possible interval and the signal is in its most compact form. The most compact form is obtained at a proper FrFT angle, which is the optimum transform angle. A chirp signal with a chirp rate m_0 has an optimal transform angle at

$$\alpha_{\text{opt}} = \arctan(m_0) + \frac{\pi}{2} + k\pi, \tag{4}$$

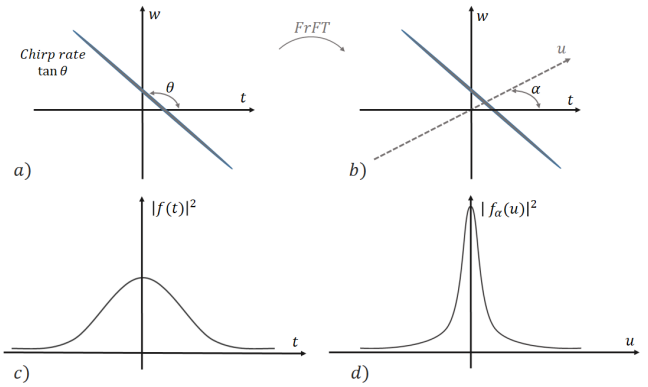

Fig. 1: The rotation and projection properties of the FrFT of a chirp signal.

where k is any integer. At this optimum angle, magnitude spectrum of the FrFT has a distinct peak [13]. For this purpose we define the following function

$$P(\alpha) = \max\left\{\left|f_\alpha\left\{c(t)\right\}(u)\right|\right\}, \tag{5}$$

which has a unique peak at the optimum angle. Moreover, as the energy distribution of a white noise is symmetric, the FrFT only concentrates the signal's energy, but energy of the noise is not concentrated. Therefore, FrFT is well suited to chirp-rate estimation problems in noisy environments. Maximum of $P(\alpha)$ yields a robust estimate of the optimum rotation angle by

$$\widehat{\alpha}_{\text{opt}} = \underset{\alpha}{\text{argmax}}\left\{P(\alpha)\right\}. \tag{6}$$

The estimated chirp rate is then easily found using

$$\widehat{m} = \tan\left(\widehat{\alpha}_{\text{opt}} - \frac{\pi}{2}\right). \tag{7}$$

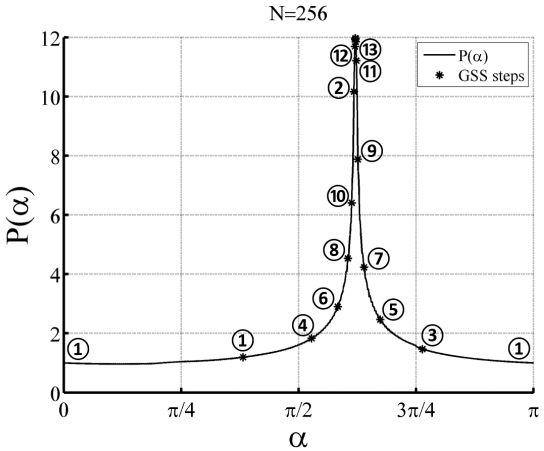

Fig. 2: Illustration of a sample $P(\alpha)$ for a chirp function in a noiseless environment. Computed GSS values are shown in the figure.

ISBN 978-0-9928626-7-1 © EURASIP 2017

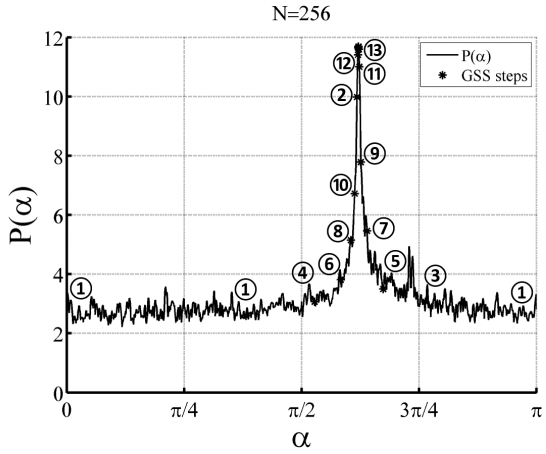

Fig. 3: Illustration of a sample $P(\alpha)$ for a chirp function in a noisy environment. Computed GSS values are shown in the figure.

Algorithm 1 GSS algorithm

$\alpha_1 \leftarrow \alpha_b - r\ (\alpha_b - \ \alpha_a\ )$,
$\alpha_2 \leftarrow \alpha_a + r\ (\alpha_b - \ \alpha_a\ )$,
$v_1 \leftarrow \ \max\{|f_{\alpha_1}\{c(t)\}(u)|\}$,
$v_2 \leftarrow \ \max\{|f_{\alpha_2}\{c(t)\}(u)|\}$,
while $|\alpha_b - \alpha_a| > \varepsilon$ **do**
  if $v_1 < v_2$ **then**
    $\alpha_a \leftarrow \alpha_1$
    $\alpha_1 \leftarrow \alpha_2$
    $\alpha_2 \leftarrow \alpha_a + r\ (\alpha_b - \ \alpha_a\ )$
    $v_1 \leftarrow v_2$
    $v_2 \leftarrow \ \max\{|f_{\alpha_2}\{c(t)\}(u)|\}$
    $\alpha_{\text{opt}} \leftarrow \alpha_2$
  else
    $\alpha_b \leftarrow \alpha_2$
    $\alpha_2 \leftarrow \alpha_1$
    $\alpha_1 \leftarrow \alpha_b - r\ (\alpha_b - \ \alpha_a\ )$
    $v_2 \leftarrow v_1$
    $v_1 \leftarrow \ \max\{|f_{\alpha_1}\{c(t)\}(u)|\}$
    $\alpha_{\text{opt}} \leftarrow \alpha_1$
  end
end

III. Estimating Chirp-Rate Using Fractional Fourier Transform and GSS

Computing the FrFT for each angle α is not practically feasible, and would cause very high computational cost. Another strategy should be adopted to avoid performing an FrFT for each value of α. We propose to use the celebrated GSS algorithm for finding the maximum value of $P(\alpha)$ which explicitly leads to the optimal angle. The GSS is a popular algorithm generally used for finding the maximum (or minimum) of a unimodal continuous function over a range $[a, b]$ without the need to compute derivatives [23]. Using GSS accelerates the search process by computing the FrFT at only certain limited angles. Error tolerance of the algorithm determines accuracy of the result.

In GSS, the cost function is evaluated at the boundaries of the search interval, e.g., $[a, b]$. Then, two points x_1, x_2 in the range $[a, b]$, are selected and the function is evaluated at these two points. If $f(x_1) < f(x_2)$, then the search interval is limited to a new range of $(x_1, b]$. Else, if $f(x_1) > f(x_2)$, the same rule is applied and the new range containing the maximum is set to $[a, x_2)$. If $f(x_1) = f(x_2)$, then the maximum lies in the new range (x_1, x_2) since the points x_1 and x_2 are on either side containing the maximum. After updating the range, one new point is selected so that the other can be reused. The values of x_1 and x_2 are selected according to $x_1^i = b^i - r\left(b^i - a^i\right)$ and $x_2^i = a^i + r\left(b^i - a^i\right)$, where $r = \frac{\sqrt{5}-1}{2}$ is the golden ratio. The obvious benefit is that each time the range is updated, one of the two test points is reused. Therefore, only one new interior point is needed and the function is evaluated additionally one more time instead of two at each iteration. The procedure is reiterated until the search interval is smaller than the desired accuracy $0 < \varepsilon \ll 1$. The last updated point is chosen as the index of the maximum value.

Figure 2 plots a sample $P(\alpha)$ for a chirp signal in noiseless case and marks the first 13 GSS steps at which $P(\alpha)$ are computed. As it is clear from the figure, the function $P(\alpha)$ is almost unimodal, which makes GSS eligible for estimating the chirp-rate. However, in a noisy environment $P(\alpha)$ is not unimodal as shown in Figure 3. Yet, it is shown in Section IV that GSS performs remarkably well under noisy conditions. This is mainly because the search steps get quickly inside the region where $P(\alpha)$ is high. In this region, the FrFT concentrates energy of the chirp, but energy of the noise is not concentrated. This is a direct consequence of the rotation property of the FrFT in time-frequency plane. The reason that the first few computed points are inside this region can be explained as follows. After alias-free sampling of chirp signals, angular chirp-rates usually decrease to smaller values. Actually, chirp-rates of sampled signals are confined between $0 \leq m \leq 1$ [24], where it corresponds to the values of optimum angle $\pi/4 \leq \alpha_{\text{opt}} \leq 3\pi/4$. Therefore, the first few points chosen by the GSS are calculated in the region where the effect of the noise is minor, compared to other regions.

Algorithm 1 summarizes the above algorithm in which the GSS is applied on $P(\alpha)$ for a signal $c(t)$, where $[\alpha_a\ \alpha_b]$ is the initial search interval. Figures 2 and 3 presents the first 13 steps for the GSS algorithm both with and without instances of noise. The total iteration number is given by

$$I = \left\lceil \frac{\log_{10}\left(\frac{\pi}{2} \times \frac{\varepsilon}{\alpha_{\text{b}} - \alpha_{\text{a}}}\right)}{\log_{10}(r)} \right\rceil, \tag{8}$$

where $\lceil \cdot \rceil$ is the ceiling function. At each iteration, we compute FrFT once. As the computational cost of FrFT is $\mathcal{O}(N \log N)$ [25] for a signal of length N, the total computational complexity of GSS is $\mathcal{O}(I \times N \log N)$.

ISBN 978-0-9928626-7-1 © EURASIP 2017

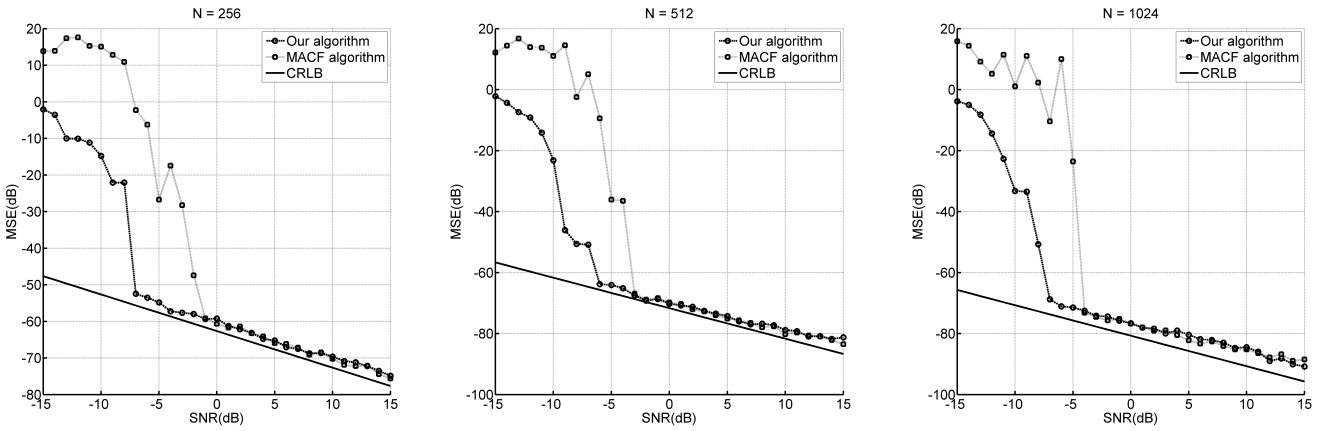

(a) (b) (c)

Fig. 4: Comparison between our algorithm and MACF for different signal lengths

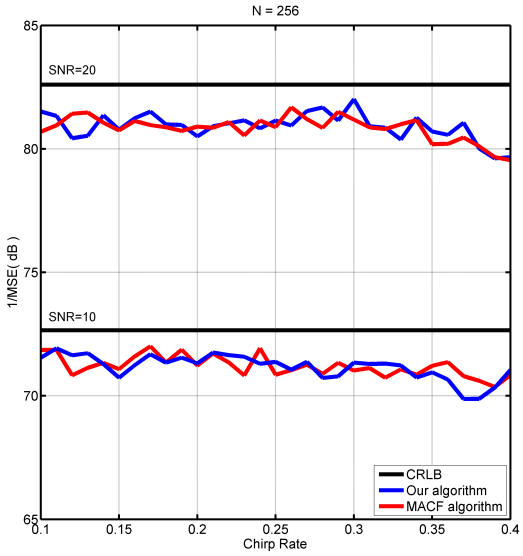

Fig. 5: Performace for different chirp rates

IV. Simulation and Results

Computer experiments have been conducted to show the efficiency of this algorithm for the chirp-rate estimation problem. A chirp signal defined in (1) is generated with the following parameters $m = 0.4$, $N = 256$ samples, $F_s = \sqrt{N}$, $f_0 = -0.1$. For the GSS, the search interval is chosen as $[0, \pi]$ and the tolerance is taken as $\varepsilon = \pi/2 \times 10^{-4}$. The experiment is conducted by changing the SNR from -15dB to 15dB with an interval of 1dB. The number of Monte Carlo simulations is set to 200 for each SNR value. We define the MSE by

$$MSE = \frac{1}{\mathrm{T}} \sum_{i=1}^{\mathrm{T}} (\widehat{m}_i - m)^2, \tag{9}$$

where $\widehat{m}_i$ is the estimated chirp rate at i-th Monte Carlo simulation and T is the total number of Monte-Carlo simulations at each SNR. Figure 4 plots the performance of the proposed algorithm for different signal lengths, 256, 512 and 1024 samples, and compares our results with Cramer-Rao lower bound (CRLB) [26] and Zheng and Shi's MACF algorithm given in [16]. The results show that the proposed method nearly achieves the CRLB for SNR values as low as -7dB. Figure 5 plots the performance of the proposed algorithm for a range of chirp rates between 0.1 and 0.4. The nearly flat results in the two SNR cases prove the validity of the proposed algorithm for a different values of chirp rates. The MACF algorithm has a computational complexity of $\mathcal{O}(63 \times N \log N)$ when the same settings given in [16] used except for the tolerance $\varepsilon = \pi/2 \times 10^{-4}$ is taken. The proposed method has a computational cost of $\mathcal{O}(21 \times N \log N)$. Therefore, the proposed algorithm is three times faster than the MACF for the same accuracy or tolerance setting. Consequently, we conclude that the proposed algorithm is faster, more accurate and more robust.

V. Conclusion

This paper presents a new method for estimating chirp rates in noisy environments. The proposed new method adopts the GSS algorithm for finding the maximum value of the FrFT in order to find the optimal angle. Simulation results prove the validity of the proposed method. The proposed method nearly achieves CRLB even for SNR values as low as -7dB, while demanding lower computational complexity. In comparison with another method, the MACF, the proposed method proves its superiority in speed, accuracy and robustness.

References

[1] A. G. Stove, "Linear FMCW radar techniques," IEE Proc. F-Radar and Signal Process., Oct. 1992, pp. 343–350, IET.

[2] P. R. Atkins, T. Collins and K. G. Foote, "Transmit-signal design and processing strategies for sonar target phase measurement," *IEEE J. Sel. Topics Signal Process.*, vol. 1, no. 1, pp. 91–104, Jun. 2007.

ISBN 978-0-9928626-7-1 © EURASIP 2017

[3] J. Muoz-Ferraras, F. Perez-Martinez and M. Burgos-Garcia, "Helicopter classification with a high resolution LFMCW radar," *IEEE Tran. Aerosp. Electron. Syst.*, vol. 45, no. 4, pp. 1373–1384, Oct. 2009.

[4] T. Misaridis and J. A. Jensen, "Use of modulated excitation signals in medical ultrasound. Part I: Basic concepts and expected benefits," *IEEE Trans. Ultrason., Ferroelect., Freq. Control*, vol. 52, no. 2, pp. 177–191, Feb. 2005.

[5] M. Martone, "A multicarrier system based on the fractional Fourier transform for time-frequency-selective channels," *IEEE Tran. Commun.*, vol. 49, no. 6, pp. 1011–1020, Jun. 2001.

[6] H. Hao, T. Xuan-ru, T. Ran, C. Xiao-kang, D. Zhao and L. Peng-fei, "Carrier tracking loop in high dynamic environment aided by fast maximum likelihood estimation of Doppler frequency rate-of-change," *J.Electron .Inf. Technol.*, vol. 36, pp. 577–582, 2014.

[7] M. Sanghadasa, P. S. Erbach, C. C. Sung, D. A. Gregory and W. A. Friday, "Wavelet transform applied to synthetic aperture radar optimal implementation and adaptive techniques," *Opt. Eng.*, vol. 33, pp. 2282–2289, Jul. 1994.

[8] R. A. Altes, "Detection, estimation, and classification with spectrograms," *J. Acoust. Soc. Amer.*, vol. 67, pp. 1232–1246, Apr. 1980.

[9] P. Rao and F. J. Taylor, "Estimation of instantaneous frequency using the discrete Wigner distribution," *Electron. Lett.*, vol. 26, pp. 246–248, Feb. 1990.

[10] J. C. Wood and D. T. Barry, "Radon transform of time-frequency distributions for analysis of multicomponent signals," *IEEE Trans. Signal Process.*, vol. 42, pp. 3166–3177, Nov. 1994.

[11] G. F. Boudreaux-Bartels, *Time-varying signal processing using the Wigner distribution*, in Advances of Geophysical Data Processing, vol. 2, M. Simaan, Ed. Greenwich, CT: JAI, 1985.

[12] C. D. Luigi and E. Moreau, "An iterative algorithm for estimation of linear frequency modulated signal parameters," *IEEE Signal Process. Lett.*, vol. 9, pp. 127–129, Apr. 2002.

[13] L. Qi, R. Tao, S. Y. Zhou and Y. Wang, "Detection and parameter estimation of multicomponent LFM signal based on the fractional Fourier transform," *Sci. China Ser. F*, vol. 47, pp. 184–198, 2004.

[14] C. Capus and K. Brown, "Fractional fourier transform of the Gaussian and fractional domain signal support," IEE Proc. Vis. Image Signal Process., Apr. 2003, vol. 150, pp. 99–106.

[15] C. Capus, Y. Rzhanov and L. Linett, "The analysis of multiple linear chirp signals," Proc. IEE Symposium on Time-Scale and Time-Frequency Analysis and Applications, Feb. 2000, vol. 4, pp. 1–7.

[16] L. Zheng and D. Shi, "Maximum amplitude method for estimating compact fractional Fourier domain," *IEEE Signal Processing Letters*, vol. 17, no. 3, pp. 293–296, Mar. 2010.

[17] H. M. Ozaktas, Z. Zalevsky and M. A. Kutay, *The fractional Fourier transform with applications in pptics and signal processing*, John Wiley, New York, USA, 2001.

[18] H. M. Ozaktas, B. Barshan, D. Mendlovic and L. Onural, "Convolution, filtering, and multiplexing in fractional Fourier domains and their relation to chirp and wavelet transforms," *J. Opt. Soc. Amer. A*, vol. 11, pp. 547–559, 1994.

[19] V. Namias, "The fractional Fourier transform and its application in quantum mechanics," *J. Inst. Maths. Applications*, vol. 25, pp. 241–265, 1980.

[20] J. R. Fonollosa and C. L. Nikias, "A new positive time-frequency distribution," Proc. IEEE Int. Con. Acoust. Speech and Signal Process., Apr. 1994, pp. IV–301–IV–304, IEEE.

[21] D. Mendlovic, H. M. Ozaktas and A. W. Lohmann, "Fractional correlation," *Appl. Opt*, vol. 34, pp. 303–309, 1995.

[22] L. B. Almeida, "The fractional Fourier transform and time-frequency representations," *IEEE Trans. Signal Process.*, vol. 42, no. 11, pp. 3084–3091, Nov. 1994.

[23] W. Cheney and D. Kincaid, *Numerical Mathematics and Computing*, Cole Publishing Company, Brooks, 3 edition, 1994.

[24] D. J. Peacock and B. Santhanam, "Comparison of centered discrete fractional Fourier transforms for chirp parameter estimation," Proc. DSP/SPE, Aug. 2013, pp. 65–68, IEEE.

[25] H. M. Ozaktas, O. Arikan, M. A. Kutay and G. Bozdagi, "Digital computation of the fractional Fourier transform," *IEEE Trans. Sig. Proc.*, vol. 44, pp. 2141–2150, Sep. 1996.

[26] S. Peleg and B. Porat, "The Cramer-Rao lower bound for signals with constant amplitude and polynomial phase," *IEEE Trans. Sig. Proc.*, vol. 39, pp. 749–752, Mar. 1991.

ISBN 978-0-9928626-7-1 © EURASIP 2017